

# Evidence for Nodal Superconductivity in LaFePO from Scanning SQUID Susceptometry

Clifford W. Hicks,<sup>1</sup> Thomas M. Lippman,<sup>1</sup> Martin E. Huber,<sup>2</sup> James G. Analytis,<sup>1</sup>  
Jiun-Haw Chu,<sup>1</sup> Ann S. Erickson,<sup>1</sup> Ian R. Fisher,<sup>1</sup> and Kathryn A. Moler<sup>1</sup>

<sup>1</sup>*Geballe Laboratory for Advanced Materials, Stanford University, Stanford, California, 94305, USA and Stanford Institute for Materials and Energy Sciences, SLAC National Accelerator Laboratory, 2575 Sand Hill Road, Menlo Park CA 94025*

<sup>2</sup>*Departments of Physics and Electrical Engineering, University of Colorado Denver, Denver, Colorado, 80217, USA*

(Dated: 2 April 2009)

PACS numbers: 74.25.Nf, 74.20.Rp

We measure changes in the penetration depth  $\lambda$  of the  $T_c \approx 6$  K superconductor LaFePO. In the process scanning SQUID susceptometry is demonstrated as a technique for accurately measuring *local* temperature-dependent changes in  $\lambda$ , making it ideal for studying early or difficult-to-grow materials.  $\lambda$  of LaFePO is found to vary linearly with temperature from 0.36 to  $\sim 2$  K, with a slope of  $143 \pm 15$  Å/K, suggesting line nodes in the superconducting order parameter. The linear dependence up to  $\sim T_c/3$  is similar to the cuprate superconductors, indicating well-developed nodes.

Research on the iron pnictide superconductors has been intense over the past year. Most attention has focused on arsenic-based materials, which have the highest transition temperatures, but which only superconduct at ambient pressure when doped, resulting in intrinsic disorder. Superconductivity in LaFePO was announced in 2006 [1]. Most likely it is the fully stoichiometric compound that superconducts, with  $T_c \approx 6$  K; very clean residual resistivities below 0.1 mΩ-cm have been obtained [2]. How similar LaFePO will prove to be to the higher- $T_c$  arsenide compounds is not clear; although LaFePO does not show the magnetic order found in the arsenide compounds, its electronic structure has been found to be very similar [3].

The temperature dependence of the penetration depth provides information on the superconducting order parameter (OP). OPs with line nodes are known to result in a  $T$ -linear dependence of  $\Delta\lambda(T) \equiv \lambda(T) - \lambda(0)$  at low  $T$  [4]. Scattering modifies this dependence to  $T^2$  [5]. A fully-gapped OP results in an exponential dependence  $\Delta\lambda \propto T^{-1/2} \exp(-T_0/T)$  [6]. For the iron pnictide superconductors, proposed OPs include nodal and nodeless  $s$  [7, 8, 9, 10, 11],  $s+d$  [12],  $p$  [13, 14] and  $d$  [8, 14, 15, 16]. Most of these predictions are based on calculations in an unfolded, 1 Fe per unit cell Brillouin zone, which neglects the avoided crossings between the electron pockets in the true zone [3]. These avoided crossings could significantly alter the nodal structure of the OP. It is also a possibility that different pnictide superconductors, although electronically similar, have different OPs [17].

Radio-frequency tunnel diode resonator and microwave

cavity perturbation measurements on iron arsenide superconductors have shown both power-law and exponential temperature dependences of  $\Delta\lambda$ . Power-law dependence has been found in  $\text{Ba}(\text{Fe}_{1-x}\text{Co}_x)_2\text{As}_2$  [18], with the exponent  $n$  varying between 2.0 and 2.6 with doping.  $n \approx 2$  has been found in  $\text{Ba}_{1-x}\text{K}_x\text{Fe}_2\text{As}_2$  [19],  $\text{NdFeAsO}_{0.9}\text{F}_{0.1}$  [20] and  $\text{LaFeAsO}_{0.9}\text{F}_{0.1}$  [20]. Exponential behavior has been found in  $\text{Ba}_{1-x}\text{K}_x\text{Fe}_2\text{As}_2$  [21],  $\text{PrFeAsO}_{1-y}$  [22] and  $\text{SmFeAsO}_{0.8}\text{F}_{0.2}$  [23].

In LaFePO, nearly linear dependence of  $\Delta\lambda$  on  $T$  to below 150 mK has been reported by Fletcher *et al* [24], using an RF tunnel diode circuit. However early LaFePO samples have had irregular shapes, which complicate RF and microwave measurements: to isolate  $\lambda_{ab}$  the magnetic field of the excitation must be specifically oriented relative to the crystal axes, and at lower frequencies knowledge of the sample size is necessary to extract  $\Delta\lambda$ . Fletcher *et al* report these slopes  $d\lambda/dT$  on three samples: 412, 436 and 265 Å/K (over  $0.7 < T < 1.0$  K). The magnitude of  $d\lambda/dT$  constrains the number and opening angle of nodes, so confirmation with additional measurement is desirable.

SQUID susceptometry has been demonstrated as a technique for observing superconducting transitions [25], and has been used to determine the Pearl length  $\Lambda$  of thin superconducting films, for  $\Lambda \sim 10\text{--}100$   $\mu\text{m}$  [26]. We extend this technique to measurement of nm-scale changes in local  $\lambda$  with varying sample temperature. Our susceptometer is a niobium-based design [28]; its front end is shown in Fig. 1. The pick-up loop is part of a SQUID, and an excitation current (in this work, at 1071 Hz) is applied to the field coil. What is measured is the field coil-pick-up loop mutual inductance  $M$ . The susceptometer chip is polished to a point, aligned at an angle relative to the sample (in this work,  $\approx 16^\circ$ ), and mounted onto a 3-axis scanner. The Meissner response of superconducting samples partially shields the field coil, so  $M$  decreases as the susceptometer approaches the sample.

The schematic in Fig. 1 shows a model of the susceptometer. The field coil is taken as a wire loop of radius  $R$  at a height  $h$  above the superconductor surface, and

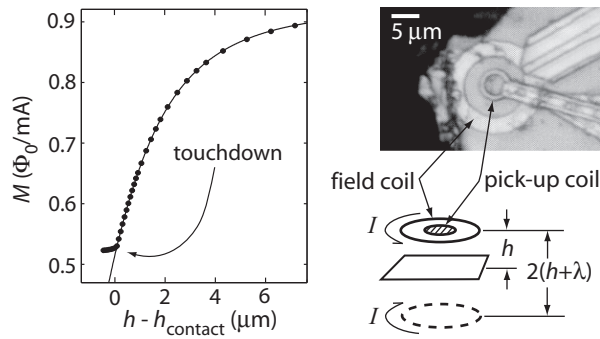


FIG. 1: Left: Field coil–pick-up loop mutual inductance  $M$  against height above the sample;  $h_{\text{contact}}$  is the height at which the corner of the susceptometer chip contacts the sample. The line is a fit of eq. 1. Right: photograph of the front end of the susceptometer, and a schematic of the susceptometer-sample geometry. The dashed loop is the image field coil.

the superconductor response field as an image coil placed a height  $2h_{\text{eff}}$  beneath the field coil, where the effective height  $h_{\text{eff}} = h + \lambda$ . The flux through the pick-up coil (radius  $a$ ) is taken as the field at its center times its area. All coils are taken parallel to the surface, neglecting the alignment angle. These approximations give a conversion between  $M$  and  $h_{\text{eff}}$ :

$$M = \frac{\mu_0}{2} \pi a^2 \left( \frac{R^2}{(R^2 + 4h_{\text{eff}}^2)^{3/2}} - \frac{1}{R} \right). \quad (1)$$

To measure changes in  $\lambda$  the susceptometer is placed in contact with a flat  $ab$ -plane area of the sample, and the sample temperature  $T$  is varied. The contact is sufficient to overcome system vibration but weak enough to avoid excessive thermal coupling (the susceptometer is maintained at  $\approx 0.3$  K). The contact keeps  $h$  constant, so changes to  $h_{\text{eff}}$  are changes in  $\lambda_{ab}$ : we are using the fact that, for  $h \gg \lambda$ , the response field of the superconductor is a function of  $h_{\text{eff}}$  alone [27]. In this sense, the physical origin of eq. 1 is irrelevant as long as it accurately models the dependence of  $M$  on  $h$ , which Fig. 1 shows to be the case.  $R$  and  $a$  are fitting parameters; they approximately match the actual dimensions of the susceptometer, but with precise values that vary with alignment angle and sample surface orientation;  $R$  and  $a$  are obtained separately for each sample. Crucial to this measurement, if the susceptometer is over a flat  $ab$  surface then the relevant penetration depth is  $\lambda_{ab}$  alone, even with nonzero alignment angle [27]. Due to the alignment angle, the minimum  $h$  is  $h_{\text{contact}} \approx 3 \mu\text{m}$ .

What is the accuracy of measurement of  $\Delta\lambda$ ? The fit to eq. 1 returns  $R$  and  $a$  consistent with a particular conversion constant, in  $\mu\text{m}/\text{V}$ , between  $h$  and applied voltage to the scanner, which is measured separately, in this work with  $\pm 5\%$  accuracy. All  $\Delta\lambda$  quoted in this work have this  $\pm 5\%$  systematic uncertainty. Also, deviations from the

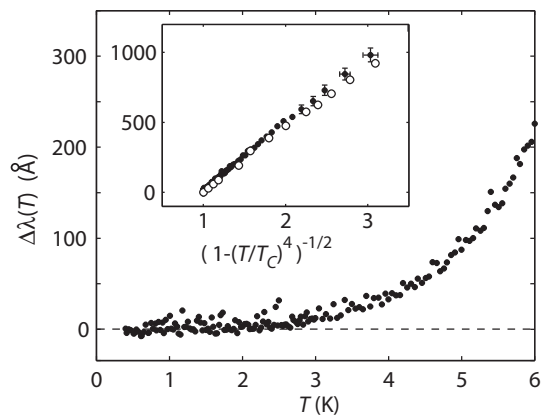


FIG. 2:  $\Delta\lambda(T) \equiv \lambda(T) - \lambda(0)$  of Pb. A drift has been subtracted as described in the text. Inset: Open symbols: measurement of Gasparovic and McLean [29]. Filled: present data; the vertical error bars are the systematic  $\pm 5\%$  error on all  $\Delta\lambda$  data in this Letter.

fit give errors on  $\Delta\lambda$  up to 1.5%. At large  $\lambda$  the assumption that the response field is a function of  $h + \lambda$  breaks down; numerical simulation shows that, at  $h = 3 \mu\text{m}$  and  $\lambda(0) = 5000 \text{ \AA}$ , this assumption leads  $\Delta\lambda$  to be underestimated by 1% at  $\Delta\lambda = 5000 \text{ \AA}$  and 4% at  $10,000 \text{ \AA}$ . Thermal gradients from the susceptometer-sample contact have minimal effect: control tests on sapphire show that the change in  $h_{\text{eff}}$  attributable to these gradients is no more than  $\sim 20 \text{ \AA}$  for  $T$  varying between 1 and 8 K. By tracking  $T_c$  of LaFePO, we determine that contact locally cools the sample by only  $\sim 40$  mK at  $T = 6$  K.

As a test we measure the penetration depth of a lump of industrial-grade lead; the results and comparison with an earlier measurement are shown in Fig. 2. A  $\sim 100 \text{ \AA}$ -scale downward drift of  $h_{\text{eff}}$ , due to the sensor gradually pressing a dent into the soft lead surface, is subtracted from our data. The drift rate is  $T$ -independent and was measured separately from the data in Fig. 2, so the flatness of  $\Delta\lambda$  at low  $T$  is real.

Fig. 3 shows the main result of this work:  $\Delta\lambda_{ab}$  vs.  $T$  for two LaFePO crystals (at the points indicated in Fig. 4(e) and (f)). For both data sets  $\Delta\lambda$  was recorded over multiple temperature sweeps, both warming and cooling, and found to follow the same path.  $\lambda$  is seen to vary nearly linearly with temperature. Fitting  $\Delta\lambda = A + BT^n$  over  $0.7 < T < 1.6$  K, from top to bottom  $n=1.22(4)$ ,  $1.13(10)$  and  $0.97(5)$  are obtained for the three curves in Fig. 3(a).

Photographs of the two LaFePO specimens are shown in Fig. 4. An example of a susceptibility scan (a scan of the spatial variation in  $M$ ) is shown in Fig. 4(c). Because  $M$  varies strongly with  $h$ , features in individual scans mainly reflect surface topography. More useful is comparison of scans at different  $T$ : e.g. Fig. 4(d) shows a map of  $h_{\text{eff}}(3 \text{ K}) - h_{\text{eff}}(0.4 \text{ K})$  on sample #2, which

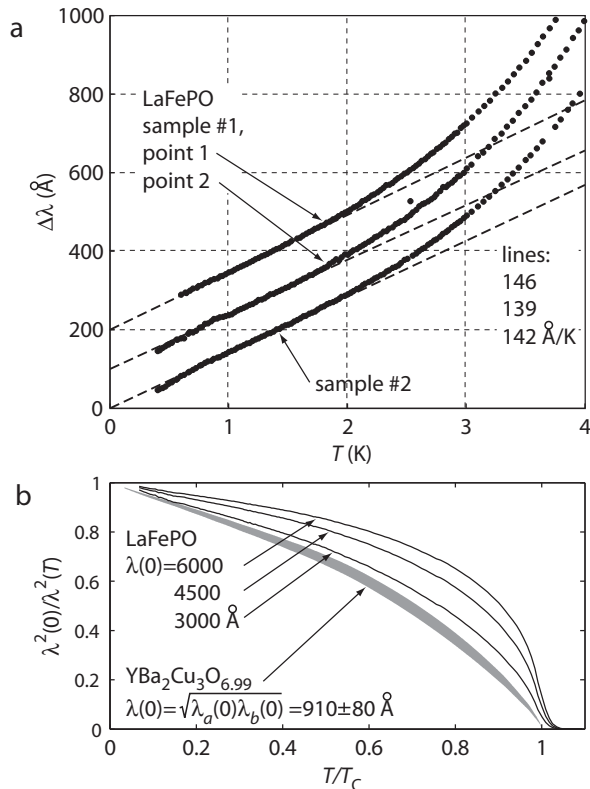


FIG. 3: Top:  $\Delta\lambda$  of two LaFePO specimens, at the points indicated in Fig. 4. The lines were fit over  $0.7 < T < 1.6$  K. Bottom: black lines are possible superfluid densities for LaFePO sample #1, point 2, with different  $\lambda(0)$ . Shaded area: superfluid density of  $\text{YBa}_2\text{Cu}_3\text{O}_{6.99}$  ( $1/(\lambda_a\lambda_b)$ ), from [30] and [31]; the width of the shaded area reflects uncertainty in  $\lambda(0)$ .

reveals two useful facts: (1) Where the sample surface is not flat  $\lambda_c$  mixes in strongly and  $\Delta h_{\text{eff}}$  is large; one needs to be at least  $\sim 10 \mu\text{m}$  from an edge to measure  $\lambda_{ab}$ . (2) Where the sample is flat, and  $\Delta h_{\text{eff}} = \Delta\lambda_{ab}$ ,  $\Delta\lambda_{ab}$  is homogeneous to within  $\sim 5\%$ ; areas of moderately increased  $\Delta h_{\text{eff}}$  are areas where the surface is pitted.

Maps of local  $T_c$ , shown in Fig. 4(e) and (f), are made by performing susceptibility scans at various  $T$  and extracting  $\Delta h_{\text{eff}}(T)$ . Most areas of the samples show weak tails of superfluid density persisting a few 0.1 K beyond the dominant local  $T_c$  (and in places beyond 7 K), which give uncertainty to estimates of the dominant  $T_c$ . Our criterion for determining local  $T_c$  is based on superfluid density: the  $\lambda(0) = 4500 \text{ \AA}$  superfluid density curve in Fig. 3(b) is taken as a reference, and in the scans the local  $\Delta h_{\text{eff}}$  is taken as  $\Delta\lambda$ . The local  $\lambda(0)$  (which varies with topography) and  $T_c$  are varied to obtain the best fit to the reference. Varying the reference  $\lambda_{ab}(0)$  by  $1000 \text{ \AA}$  varies the calculated  $T_c$ 's by  $\sim 0.1$  K.

$\lambda(0)$  could in principle be extracted from the geometry of the susceptometer and its contact with the sample surfaces; however the uncertainties are large. From the

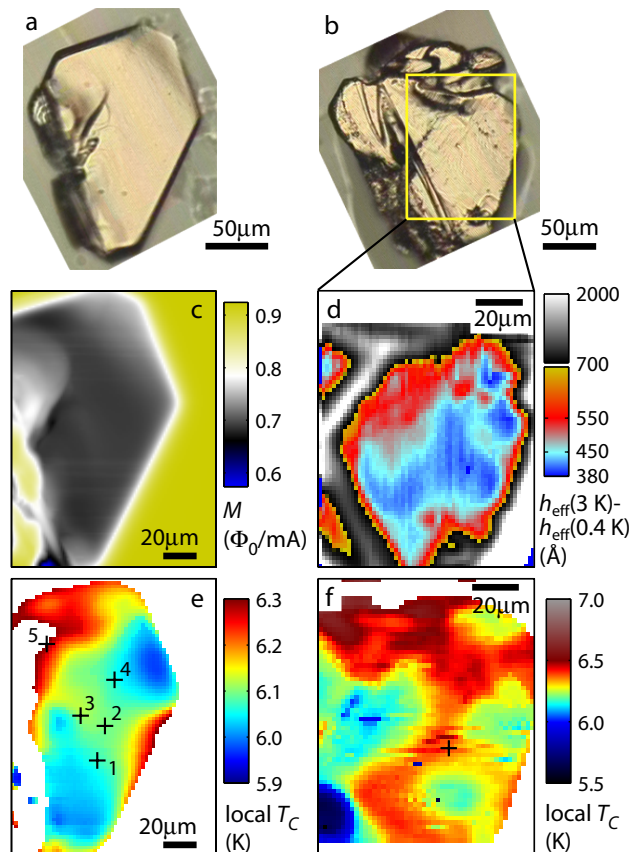


FIG. 4: (a,b) LaFePO specimens #1 and #2. (c) Susceptibility scan of #1 at  $T = 0.4$  K. Over the superconductor  $M$  is reduced from its vacuum level by the Meissner response. (d) Change in  $h_{\text{eff}} = h + \lambda$  between 0.4 and 3 K over specimen #2. (e,f) Maps of local  $T_c$ , over the same areas as in (c) and (d). The crosses indicate the points where  $\Delta\lambda(T)$  data were collected.

variation of  $M$  with surface orientation and SEM images of the susceptometer a plausible contact point on the susceptometer can be identified, and comparison with the lead specimen indicates that  $\lambda_{ab}(0)$  of LaFePO likely falls in the range  $3500\text{--}5500 \text{ \AA}$ .

At the five points on sample #1 indicated in Fig. 4(e),  $d\lambda/dT$  over the linear portion of  $\Delta\lambda$  is 146, 139, 136, 150 and 205  $\text{\AA}/\text{K}$ , and at the single measurement point on sample #2, 142  $\text{\AA}/\text{K}$ . The 205  $\text{\AA}/\text{K}$  measurement was at a point with significant topography and can be excluded. Taking into account the 5% and 1.5% uncertainties,  $d\lambda/dT$  is  $143 \pm 15 \text{ \AA}/\text{K}$ .

The superfluid densities  $\rho_S \equiv 1/\lambda^2$  of LaFePO and  $\text{YBa}_2\text{Cu}_3\text{O}_{6.99}$  are compared in Fig. 3. The linear portion of  $\rho_S$  persists to a similar fraction of  $T_c$  in both materials, indicating that the nodes in LaFePO must be well-formed, as in  $\text{YBa}_2\text{Cu}_3\text{O}_{6.99}$ —the magnitude of the gap on either side of the nodes must be similar. In contrast, accidental nodes in nodal  $s$  orders may result in very asymmetric + and - lobes [32]. Also apparent in Fig. 3

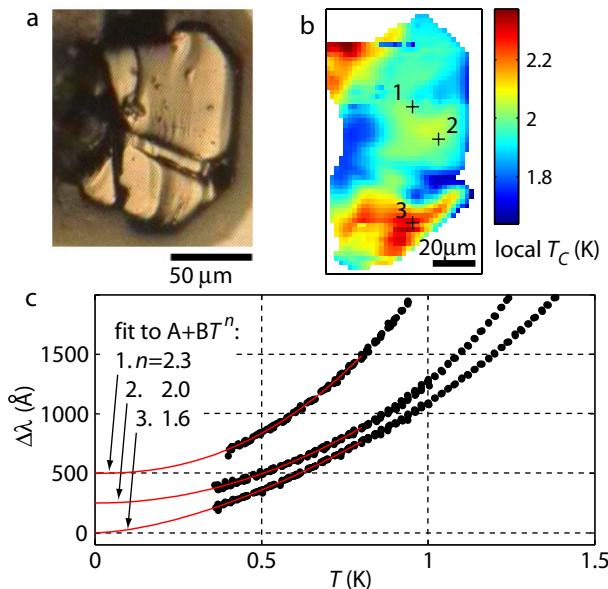


FIG. 5: (a) Photograph and (b) map of local  $T_c$  of a  $T_c \approx 2$  K specimen. The relative error on local  $T_c$ 's is  $\sim 0.1$  K. (c)  $\Delta\lambda(T)$  at the three points indicated in (b). Because the sample surface is not flat, these measured  $\Delta\lambda$  include some fraction of  $\lambda_c$ .

is that  $\rho_S$  of LaFePO rises very sharply on cooling just below  $T_c$ . If the pairing is mediated by magnetic fluctuations then such a sharp rise may result from a gapping-out of low-frequency, pair-breaking fluctuations [33].

An intriguing possibility of highly asymmetric nodal  $s$  orders is that scattering might lift the nodes altogether, resulting in exponential rather than  $T^2$  dependence of  $\Delta\lambda$  at low  $T$  [32]. In this work we also studied a  $T_c \approx 2$  K LaFePO specimen. The reason for the anomalously low  $T_c$  is unclear; electron probe microanalysis shows no impurities (to the  $\frac{1}{2}\%$  level), and no anomalies in the La, Fe and P concentrations (to within  $\frac{1}{2}$ ,  $\frac{1}{2}$ , and 2%).

Fig. 5 a shows the 2 K specimen. Compared with the 6 K samples  $T_c$  varies more widely both on large and small length scales: at each point studied strong tails of superfluid density extend well above the dominant local  $T_c$ .  $\Delta\lambda$  versus temperature was recorded at three locations. Fitting to a power law over  $T < 0.8$  K, exponents  $n=2.3\pm 0.1$ ,  $2.0\pm 0.1$  and  $1.6\pm 0.1$  are obtained. The dominant local  $T_c$ 's at these three locations are  $2.1\pm 0.2$ ,  $2.0\pm 0.1$  and  $2.5\pm 0.1$  K, respectively; deviations from  $n=2$  may in part reflect variation in the local  $T_c$  (or local  $T_c$  distribution). On data up to 0.8 K, power law fits perform better than exponential fits. Within our precision and temperature limits,  $\Delta\lambda(T)$  is consistent with dirty nodal superconductivity, and with many of the measurements on As-based materials.

In conclusion, we have observed a linear temperature dependence of  $\Delta\lambda_{ab}(T)$  below  $\sim T_c/3$  in LaFePO and

accurately measured its slope,  $143\pm 15$  Å/K, using a local technique. The large temperature range of linear  $\lambda_{ab}(T)$  indicates well-formed nodes.

This work was funded by the United States Department of Energy (DE-AC02-76SF00515). We thank Douglas Scalapino, John Kirtley, David Broun, Vladimir Kogan and Walter Hardy for useful discussions.

- [1] Y. Kamihara *et al*, J. Amer. Chem. Soc. **128** (2006) 10012.
- [2] J.G. Analytis *et al*, cond-mat/08105368.
- [3] A.I. Coldea *et al*, Phys. Rev. Lett. **101** (2008) 216402.
- [4] J. Annett, N. Goldenfeld and S.R. Renn, Phys. Rev. B **43** (1991) 2778.
- [5] P.J. Hirschfeld and N. Goldenfeld, Phys. Rev. B **48** (1993) 4219.
- [6] M. Tinkham, *Introduction to Superconductivity*, 2<sup>nd</sup> ed. (McGraw-Hill, New York, 1996).
- [7] I.I. Mazin, D.J. Singh, M.D. Johannes and M.H. Du, Phys. Rev. Lett. **101** (2008) 057003.
- [8] K. Kuroki *et al*, Phys. Rev. Lett. **101** (2008) 087004.
- [9] Fa Wang, Hui Zhai, Ying Ran, A. Vishwanath and D.H. Lee, Phys. Rev. Lett. **102** (2009) 047005.
- [10] W.Q. Chen, K.Y. Yang, Yi Zhou and F.C. Zhang, Phys. Rev. Lett. **102** (2009) 047006.
- [11] A.V. Chubukov, D.V. Efremov and I. Eremin: Phys. Rev. B **78** (2008) 134512.
- [12] Kangjun Seo, B.A. Bernevig and Jiangping Hu: Phys. Rev. Lett. **101** (2008) 206404.
- [13] P.A. Lee and X.G. Wen, Phys. Rev. B **78** (2008) 144517.
- [14] X.L. Qi, S. Raghu, C.X. Liu, D.J. Scalapino, S.C. Zhang: cond-mat/08044332.
- [15] Q.M. Si and E. Abrahams: Phys. Rev. Lett. **101** (2008) 076401.
- [16] Z.J. Yao, J.X. Li and Z.D. Wang, New J. Phys. **11** (2009) 025009.
- [17] S. Graser, T.A. Maier, P.J. Hirschfeld and D.J. Scalapino, New J. Phys. **11** (2009) 025016.
- [18] R.T. Gordon *et al*, Phys. Rev. B **79** (2009) 100506(R).
- [19] C. Martin *et al*, cond-mat/09021804.
- [20] C. Martin *et al*, cond-mat/09032220.
- [21] K. Hashimoto *et al*, cond-mat/08103506.
- [22] K. Hashimoto *et al*, Phys. Rev. Lett. **102** (2009) 017002.
- [23] L. Malone *et al*, cond-mat/08063908.
- [24] J.D. Fletcher *et al*, cond-mat/08123858.
- [25] B.W. Gardner *et al*, Rev. Sci. Instr. **72** (2001) 2361.
- [26] F. Tafuri, J.R. Kirtley, P.G. Medaglia, P. Orgiani and G. Balestrino, Phys. Rev. Lett. **92** (2004) 157006.
- [27] V.G. Kogan, Phys. Rev. B **68** (2003) 104511.
- [28] M.E. Huber *et al*, Rev. Sci. Instrum. **79** (2008) 053704.
- [29] R.F. Gasparovic and W.L. McLean, Phys. Rev. B **2** (1970) 2519.
- [30] D.A. Bonn and W.N. Hardy, in *Handbook of High-Temperature Superconductivity*, edited by J.R. Schrieffer (Springer, New York, 2007).
- [31] T. Pereg-Barnea *et al*, Phys. Rev. B **69** (2004) 184513.
- [32] V. Mishra *et al*, Phys. Rev. B **79** (2009) 094512.
- [33] P. Monthoux and D.J. Scalapino, Phys. Rev. B **50** (1994) 10339.